KSTLE International Journal, Vol. 1, No. 2, December 2000, pp. 107-112

Characteristics of a Coupled Gas Lubricated Bearing for a Scaled-Up Micro Gas Turbine

Yong-Bok Lee†, Hyunduck Kwak, Chang-Ho Kim and Gunhee Jang*

Tribology Research Center, Korea Institute of Science and Technology
**Department of Precision Mechanical Engineering, Hanyang University*

Abstract: In case of the limitation of Deep RIE fabrication for Micro Gas Turbine, bearing aspect ratio is limited in very small value. The characteristics such as pressure distribution, load capacity and non-linearity of a short bearing of L/D=0.083 and a conventional bearing of L/D=1.0 with coupled boundary effects are investigated for Micro Gas Turbine bearings. The coupled effect was analyzed by mass conservation at coupled end area. The results, increasing load capacity and non-linearity due to the coupled effect of thrust and journal bearing, are obtained and the selection of journal bearing type is discussed.

Key words: micro gas turbine, L/D ratio, slip flow, load capacity, non-linearity

Introduction

As the development of micromaching progresses, the focus of study of MEMS (Micro Electro-Mechanical System) moves from static devices to dynamic devices. Naturally, a strong requirement of development of power device that provides a sufficient energy to dynamic device has been grown. Typically, power devices used in the dynamic devices have low efficiency, and it has been a major obstacle for developing various dynamic devices. Table 1 shows a comparison of efficiency of various power devices for dynamic devices.

As shown in Table 1, the micro combustion system has a very good specific power ratio and could be a possible candidate solution for the power device.

Thus studies on the micro combustion system are widely performed. Specially, a study of Micro Gas Turbine have been performed by Micro Gas Turbine Team at MIT [2,3].

Because micromachining technology is a continuous process of chemical reaction such as addition, subtraction, modification, patterning and fabrication of materials, there exist some differences from typical machining. The most important difference is a limit of aspect ratio of structure. This means that the bearing geometry is limited by its manufacturing technology. Actually, it is impossible to manufacture a bearing with high L/D ratio and using a low L/D ratio bearing for Micro Gas Turbine could not be avoided.

For that kind of bearing which attempt to use for Micro Gas Turbine, Dr. Orr studied the stability characteristics of gas lubricated bearings with very low L/D (0.075) ratio by using Galerkin method, and showed that there is not only whirl instability but also radial instability [4].

Fig. 1 shows a cut-away view of rotor and bearing. The bearing consists of three pieces, upper thrust pad, journal pad and lower thrust pad, which has four pressure feeding holes with 100 μm radius. Each hole was connected with an external compressor. And two types of journal pad were manufactured, and one has feeding holes, while the other has no feeding holes for the comparison between hydrodynamic and externally pressurized journal bearing, while thrust pad always has feeding holes.

When the rotor runs, the compressor will inhale the air from atmosphere. And it is expected that the inhaled air could be used to support bearing. For use of the air, each bearing pad has feeding holes from the compressor chamber to the bearing surface.

It should be noted that the journal bearing has an extremely low L/D ratio about 0.083 due to the limitation of micromachining technology and also noted that thrust and journal bearings are coupled each other. Seeing circle A in Fig. 1 each end of thrust and journal bearing is coupled. It is expected that this coupled effect of both bearings will have an influence on bearing behavior.

Table 1. Comparison of power density of micro power devices [1].

Device	Power Density(MW/m^3)
Micro-Lithium battery	0.4
Micro solar cell	1
Micro-elastic motor	1.7
Micro-reactor	20
Large scale combustor	40
Micro channel reactor	150
Micro-magnetic reactor	200
Micro-combustor	2000

†Corresponding author; Tel: 82-2-958-5663, Fax: 82-2-958-5659
E-mail: lyb@kistmail.kist.re.kr

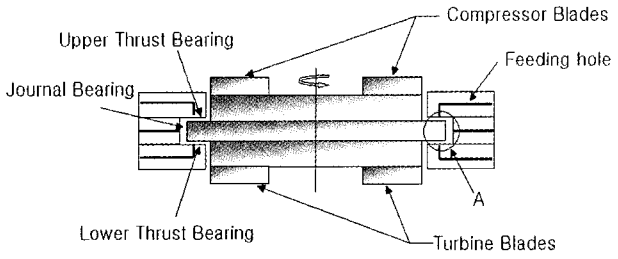

Fig. 1. Cut-away view of rotor and bearing.

The motivation behind this study is to investigate an extremely short journal bearing behavior of coupled boundary effect with thrust bearing. Additionally, for the selection of suitable journal bearing, results of hydrodynamic and externally pressurized journal bearing were investigated.

Theoretical Analysis

Validity of Reynolds Equation

In real Micro Gas Turbine, in order to provide a sufficient compressor pressure ratio, rotor runs extremely high speed. Based on technical report of KIST, its speed is almost 2,000,000 rpm [5] If the rotor diameter of real Micro Gas Turbine is to be 4 mm, its DN value (diameter times the number of revolution) is 8,000,000. However for the scaled-up Micro Gas Turbine test rig, its rotor diameter is 12 mm. For the same DN value with real Micro Gas Turbine, the rotor of test rig should rotate about 670,000 rpm.

The Reynolds number in fluid film lubrication is expressed as follows.

$$\mathrm{Re} = \frac{inertia}{viscous} = \frac{\rho_0 u_0 c_0}{\mu_0} \tag{1}$$

ρ_0, u_0, c_0 and μ_0 are force density, characteristic velocity, reference film clearance and absolute viscosity, respectively. When the rotor of the test rig rotates about 670,000 rpm, Reynolds number of thrust and journal bearing of test rig is less than unity. Thus laminar flow assumption could be taken.

Before taking Reynolds equation as a governing equation, its minimum fluid film thickness should be also considered. If the film thickness of the bearing were small enough to reach the arbitrary ratio compared to the mean free molecular path of gas, the gas slips on the bearing surface, so called slip flow is occurred [6,7]. In slip flow the velocity profile through the film is different from that seen in laminar flow. In slip flow a difference exists between surface velocity and average fluid velocity at the surface. Thus when slip flow occurs, Reynolds equation does not hold its validity anymore. The Knudsen number Kn is an inverse measure of the average number of molecular collisions, which is given as follows

$$Kn = \frac{\lambda_m}{h} \tag{2}$$

λ_m is mean free molecular path of gas and h is film thickness.

If Kn is less than 0.01, the flow may be treated as laminar flow, while slip flow becomes significant if Kn is greater than 0.01 The typical λ_m of air is 0.064 μm and h varies from 0 μm to 12 μm due to change of eccentricity ratio of journal bearing. Therefore when the film thickness is smaller than 6.4 μm, the slip flow should not be ignored and Reynolds equation could not be used as a governing equation.

Thus in this paper, all results are on the baseline that the eccentricity ratio is not greater than 0.5 in order to hold a validity of Reynolds equation and the results including slip flow remain as further work.

Analysis Method

The generalized Reynolds equation for compressible lubricant is written as follows.

$$\frac{\partial}{\partial \chi}\left(\frac{\rho h^3}{12\mu}\frac{\partial p}{\partial \chi}\right) + \frac{\partial}{\partial y}\left(\frac{\rho h^3}{12\mu}\frac{\partial p}{\partial y}\right) = \frac{U}{2}\frac{\partial(\rho h)}{\partial x}$$

And assuming that air is perfect gas, the relation $\rho = p/RT$ can be applied. The Reynolds equation for compressible, isoviscous fluid can be expressed as follows.

$$\frac{\partial}{\partial \chi}\left(ph^3\frac{\partial p}{\partial \chi}\right) + \frac{\partial}{\partial y}\left(ph^3\frac{\partial p}{\partial y}\right) = \Lambda\frac{\partial(\rho h)}{\partial x} \tag{3}$$

$$\frac{\partial}{\partial r}\left(rph^3\frac{\partial p}{\partial r}\right) + \frac{1}{r}\frac{\partial}{\partial \theta}\left(ph^3\frac{\partial p}{\partial \theta}\right) = \Lambda\frac{\partial(\rho h)}{\partial \theta} \tag{4}$$

Equation (4) is expressed in cylindrical coordinates. And Λ is bearing number.

Equation (3) and (4) are in nonlinear elliptical partial differential form and can be written in vector form as follows

$$\nabla \cdot (ph^3\nabla p - \Lambda(ph)) = 0 \tag{5}$$

$$\nabla \cdot \left(ph^3\frac{\partial p}{\partial r} - \frac{ph^3}{r}\frac{\partial p}{\partial \theta} - \Lambda(rph)\right) = 0 \tag{6}$$

After integrating equation (5) and (6) about the surface at each node and applying Gauss divergence theorem, then these equations can be transformed into line integral. And a discretization about four surfaces at arbitrary node is applied. Finally, the algebra equations at each node are obtained, and these sets of equations could be solved numerically by iterations. The set of equations of journal bearing can be expressed as follows at arbitrary node.

$$(A_1+A_2+A_3+A_4)p_{i,j} = A_1p_{i+1,j}+A_2p_{i,j+1}+A_3p_{i-1,j}+A_4p_{i,j-1}-A_5+A_6 \tag{7}$$

where

$$A_1 = \frac{p_{i+1/2,j}}{2\Delta x_{i+1}}(h^3_{i+1/2,j+} \cdot \Delta y_{j+1} + h^3_{i+1/2,j-} \cdot \Delta y_j)$$

$$A_2 = \frac{p_{i,j+1/2}}{2\Delta y_{i+1}}(h^3_{i+,j+1/2} \cdot \Delta x_{i+1} + h^3_{i-,j+1/2} \cdot \Delta x_i)$$

$$A_3 = \frac{p_{i-1/2,j}}{2\Delta x_i}(h^3_{i-1/2,j+} \cdot \Delta y_{j+1} + h^3_{i-1/2,j-} \cdot \Delta y_j)$$

$$A_4 = \frac{p_{i,j-1/2}}{2\Delta y_j}(h^3_{i+,j-1/2} \cdot \Delta x_{i+1} + h^3_{i-,j-1/2} \cdot \Delta x_i)$$

$$A_5 = \frac{\Lambda \cdot p_{i+1/2,j}}{2}(h_{i+1/2,j+} \cdot \Delta y_{j+1} + h_{i+1/2,j-} \cdot \Delta y_j)$$

$$A_6 = \frac{\Lambda \cdot p_{i-1/2,j}}{2}(h_{i-1/2,j+} \cdot \Delta y_{j+1} + h_{i-1/2,j-} \cdot \Delta y_j)$$

Simultaneously, equation (6) can be expressed in algebra form.

Additionally, in order to consider feeding holes, external flow rate Qs is added in right side of equation (7) at the each node where feeding holes are located.

Mass Conservation at Coupled End

Fig. 2 shows the coordinates of bearings. y direction, r direction and direction represent the axial direction of journal bearing, radial direction of thrust bearing and circumferential direction of both bearings, respectively.

To couple thrust and journal bearing, continuity condition of mass flow rate at coupled point is applied, that is, mass flow rate must be maintained in a coupled control volume.

Fig. 3 is a view in detail of circle A in Fig. 3. In Fig. 3, H_T and H_J are the film thickness of thrust and journal bearing, respectively. And $\dot{m}_r$ and $\dot{m}_y$ are mass flow rate along the r-direction and y-direction, p_o is pressure at coupled control volume. Finally, $p_T(r, \theta)$ and $p_J(y, \theta)$ are the pressure at each node along the thrust and journal bearing. For applying the continuity condition, two assumptions were taken.

1. Mass flow rate along r and y direction is maintained at the coupled end.
2. There is no pressure drop at the coupled end.

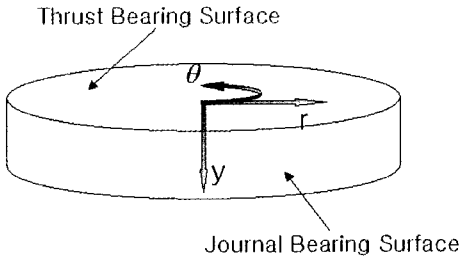

Fig. 2. Coordinates.

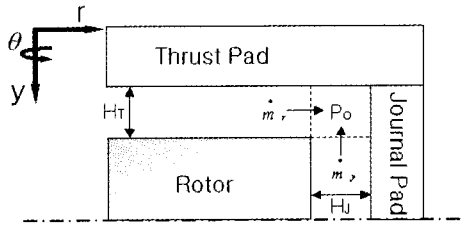

Fig. 3. Mass flow in a coupled control volume.

The assumption 1 means any mass flow along r or y axis does not dissipate in θ direction and this assumption can be valid because it was shown that the flow rate of r or y axis is much larger than that of θ axis for short bearing [7].

The assumption 2 means that the pressure at journal bearing end has the same value with the pressure at thrust bearing end. By applying the continuity conditions, following relation can be used.

$$\dot{m}_r + \dot{m}_y = 0 \tag{8}$$

These mass flow rates can be expressed as follows.

$$\dot{m}_r = -\rho\frac{H^3_T}{12\mu}\frac{\partial p_T}{\partial r} = -\frac{p_T(r, \theta)H^3_T}{12\mu RT}\frac{\partial p_T}{\partial r} \tag{9}$$

$$\dot{m}_y = -\rho\frac{H^3_J}{12\mu}\frac{\partial p_J}{\partial y} = -\frac{p_J(y, \theta)H^3_T}{12\mu RT}\frac{\partial p_J}{\partial y} \tag{10}$$

$\rho = p/RT$ relation was used in equation (9) and (10).

Substitute equation (9) and (10) into equation (8), following equation is obtained.

$$H^3_T\frac{\partial p_T}{\partial r} + H^3_J\frac{\partial p_J}{\partial y} = 0 \tag{11}$$

Remaining work of equation (11) is a descretization process which is shown as follows.

$$\frac{\partial p_T}{\partial r} = \frac{p_T(r_{end}, \theta) - p_T(r_{end} - 1, \theta)}{\Delta r} \tag{12}$$

$$\frac{\partial p_J}{\partial y} = \frac{p_J(y_{end}, \theta) - p_J(y_{end} - 1, \theta)}{\Delta y} \tag{13}$$

After substituting equation (12) and (13) into equation (11) and by applying the assumption that there is no pressure drop at the coupled end, $p_T(r_{end},\theta) = p_J(y_{end},\theta) = p_0$, equation (11) becomes an algebra form.

$$p_0 = \frac{1}{h^3_T/\Delta r + h^3_J/(\Delta y)} \cdot \left[\frac{h^3_T}{\Delta r}p_T(r_{end} - 1, \theta) + \frac{h^3_J}{\Delta y}p_J(y_{end} - 1, \theta)\right] \tag{14}$$

Thus equation (7) can be solved by iteration while applying equation (14) at the coupled boundary of each bearing.

Results and Discussion

Table 2 shows the properties of scaled-up Micro Gas Turbine test rig. The test rig was manufactured three times larger than real system because of easy maintenance and measurement. Although it is three times larger, it is expected to be a successful approach to investigate major characteristics of short and coupled bearing. It is noted that the test rig was manufactured so that the journal bearing has an extremely low

Table 2. properties of micro gas turbine test rig.

Rotational speed	670,000 rpm
Thrust film clearance	20 μm
Journal film clearance	12 μm
Diameter of rotor	10 mm
Diameter of journal bearing	12 mm
Length of journal bearing	1 mm
L/D ratio of journal bearing	0.083

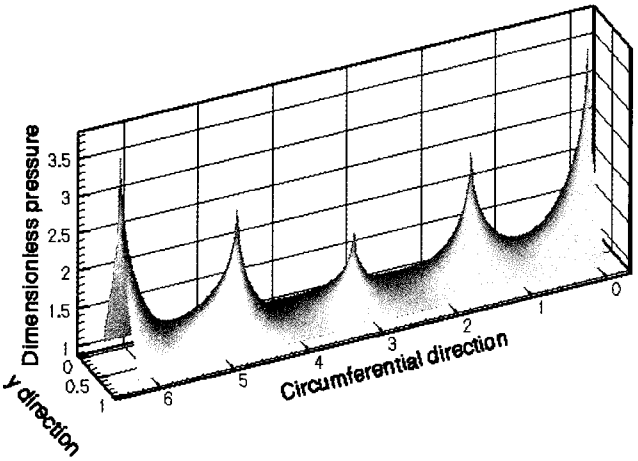

Fig. 4. pressure distribution of journal bearing externally pressurized, four feeding holes, L/D = 1.0, pressure ratio of jounal = 4.0, eccentricity ratio = 0.5 uncoupled.

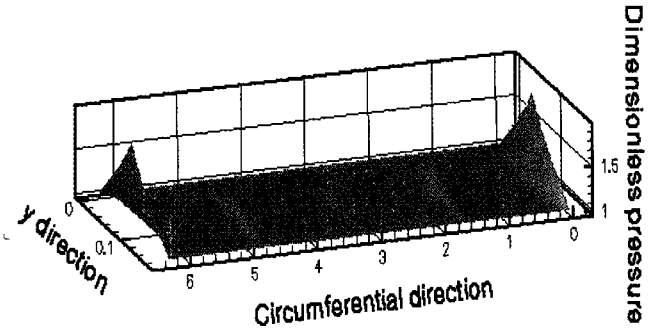

Fig. 5. pressure distribution of journal bearing externally pressurized, four feeding holes, L/D = 0.083, pressure ratio of jounal = 4.0, eccentricity ratio = 0.5 uncoupled.

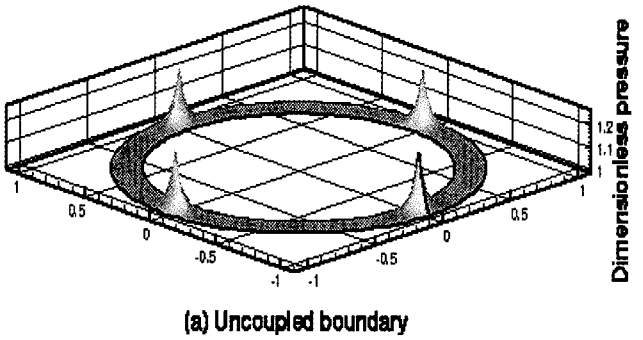

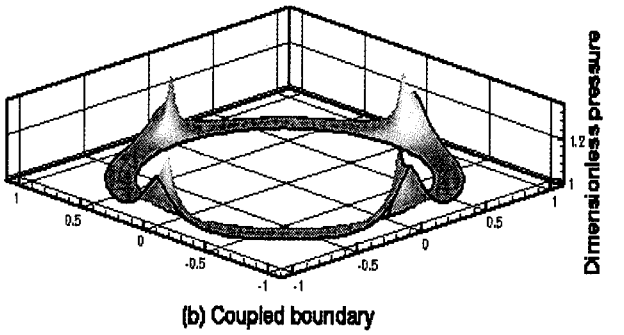

Fig. 6. pressure distribution of thrust bearing externally pressurized, four feeding holes, pressure ratio of thrust and jounal = 4.0.

L/D ratio, 0.083

Fig. 4 and 5 show the pressure distribution of externally pressurized journal bearing correspond to L/D = 1 and L/D = 0.083 The analysis was performed, as a typical case, by setting the boundary pressure equals to ambient pressure P_a

As shown in Fig. 4 and 5, a significant difference between two L/D ratios was observed. For a conventional bearing, in case of L/D = 1.0, pressure distributions in circumferential and y direction are both considerable. In Fig. 4, pressure is well-distributed in circumferential and y direction. However for a special case of bearing which is very short, L/D = 0.083, pressure distribution in the circumferential direction is less significant than that in the y direction. This means that flow in y direction induced by pressure, i.e., Poiseuille flow, is much larger than that in circumferential direction. The assumption 1 was taken in this manner. As shown in Fig. 5, pressure is mainly generated in y direction near feeding holes. Between feeding holes, pressure gradient is almost zero in circumferential direction.

If interaction between thrust and journal bearing were considered, it should be expected that the pressure at coupled end slightly increases compared to the ambient pressure. Thus load capacity of thrust and journal bearing will be expected to increase because load capacity is the sum of pressure on bearing surface.

Fig. 6 shows a comparison of thrust bearing pressure distribution in two cases, coupled and uncoupled boundary case. Coupled boundary means that interaction between thrust and journal bearing was considered, while uncoupled boundary means that boundary condition was set as ambient pressure.

Clearly, if the interaction between thrust and journal bearing is considered, load capacity of bearing will increase. As shown in coupled boundary case in Fig. 6, pressure near the outer side, at the coupled boundary, was increased compared to the uncoupled boundary case. This phenomenon increases the sum of pressure on bearing surface, so that the load capacity of bearing increases.

This result means that pressure of thrust bearing has an effect on hydrodynamic journal bearing direct and, even in hydrodynamic case, journal bearing will behave like an externally pressurized bearing.

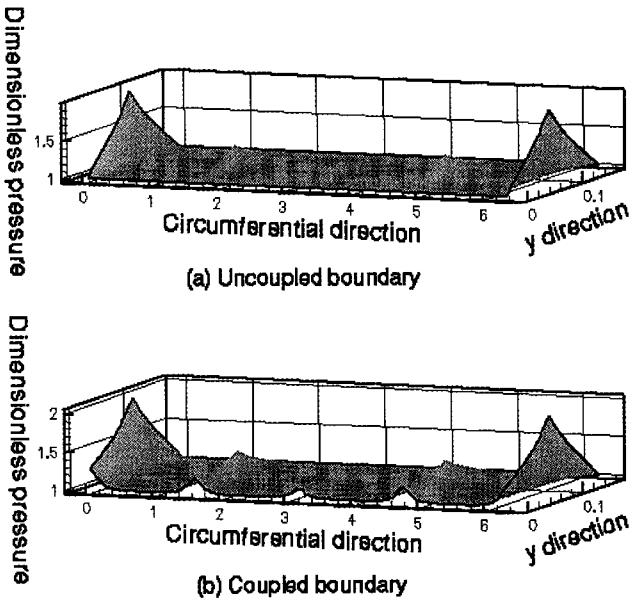

Fig. 7. Pressure distribution of journal bearing externally pressurized, four feeding holes, L/D = 0.083, pressure ratio of thrust and jounal = 4.0, eccentricity ratio = 0.5.

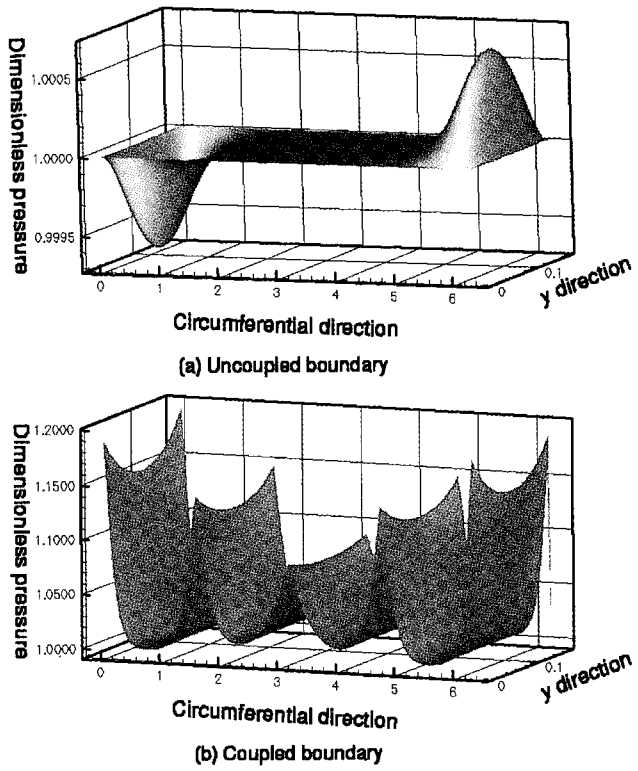

Fig. 8. pressure distribution of journal bearing hydrodynamic, L/D = 0,083, eccentricity ratio = 0.5.

It should be noted that the coupled journal bearing is very sensitive to the thrust bearing in hydrodynamic case. If the pressure distribution of the thrust bearing is suddenly perturbed, the pressure distribution of journal bearing is also perturbed. Actually, in real operating condition, pressure distribution of thrust bearing may vary dynamically and this

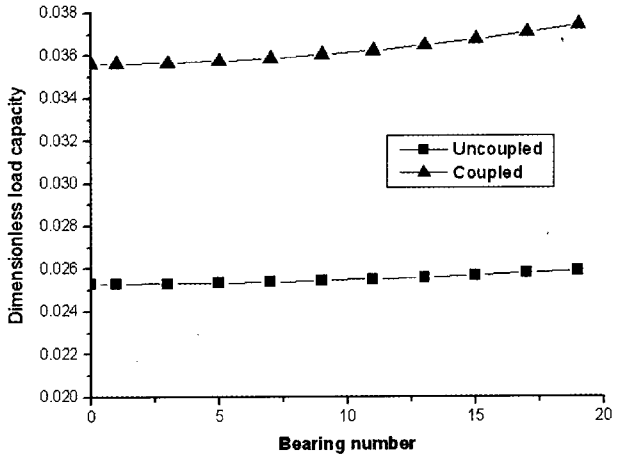

Fig. 9. Dimensionless load capacity vs. bearing number of jounal bearing externally pressurized, four feeding holes, L/D = 0.083, pressure ratio = 4.0, eccentricity ratio = 0.5.

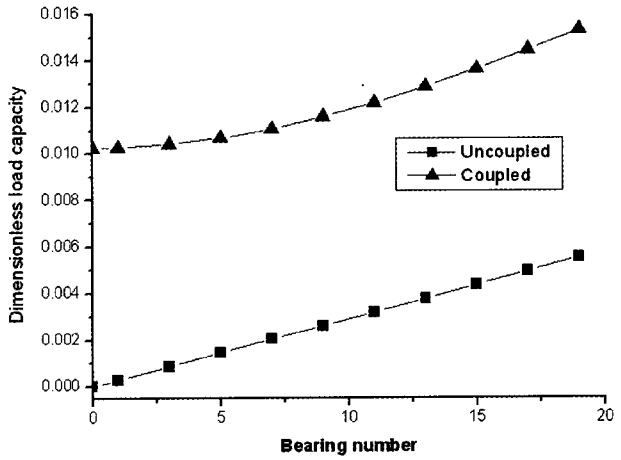

Fig. 10. Dimensionless load capacity vs. bearing number of jounal bearing hydrodynamic, holes, L/D = 0.083, pressure ratio = 4.0, eccentricity ratio = 0.5.

could make an undesirable situation to journal bearing.

Fig. 9 shows the dimensionless load capacity vs. bearing number curve of externally pressurized journal bearing case. Clearly, load capacity of journal bearing increases when the interaction between thrust and journal is considered. The load capacity of uncoupled externally pressurized journal bearing increases slightly due to increasing bearing number, and its trend is linear as shown. Also load capacity of coupled externally pressurized journal bearing increases slightly with nonlinear trend. The gradient of load capacity curve slightly increase as bearing number is larger.

Simultaneously, dimensionless load capacity vs. bearing number curve of hydrodynamic journal bearing case is shown in Fig. 10 Fig. 10 shows similar trend with externally pressurized journal bearing case. However it is noted that non-linearity of coupled case is more significant than that of externally pressurized journal bearing case. As shown in Fig. 10, load capacity of coupled case increase rapidly compared to coupled case of externally pressurized journal bearing. This

means, as described above, journal bearing is more sensitive to thrust bearing than that of externally pressurized case. Under real operating situation, various kind of disturbance will affect system and it is desirable that system is less sensitive to such disturbance.

On this concept, externally pressurized journal bearing type is recommendable compared to hydrodynamic journal bearing type because it is less sensitive to its high load capacity. However, in externally pressurized journal bearing type, a pressure source could be a problem. That means, the inhaled air from compressor can be used for the pressure source of both journal and thrust bearings, however such design reduces the amount of air used in combustion and it could induce a decreasing of efficiency of combustion. Therefore in order to select a type of journal bearing, a close and careful investigation of possibility of using inhaled air from compressor may be needed.

Conclusion

In this paper, the characteristics of gas lubricated bearing, such as non-linearity and load capacity, are discussed, based on the successful direct numerical method in Micro Gas Turbine. The characteristics of very short bearing with a coupled boundary effect which increases a load capacity and induces a non-linearity are observed. However all results in this paper are limited in eccentricity ratio less than 0.5 because Reynolds equation does not hold its validity in large eccentricity ratio region. In that region slip flow of gas must be considered and it remains as further work.

Acknowlegment

This work was supported by a grant from the Critical Technology 21 Project of the Ministry of Science and Technology, Korea.

References

1. Dae-Hoon Lee, Sejin Kwon, Ki-Chul Chun, Euisik Yoon and Chol Hee Han, Micro Combustion Phenomena and Combustion Device Development, 2000 Proceeding of the 2nd Korean MEMS Conference, pp. 211-217
2. Ian A. waitz, Guatam Guaba and Yang-Sheng Tzeng, Combustors for Micro-Gas Turbine Engines, Journal of Fluids Engineering, Vol. 120, pp. 109-117, 1998
3. E. S. Piekos and K. S. Breuer, Pseudospectral Orbit Simultaion of Nonideal Gas-Lubricated Journal Bearings for Microfabricated Turbomachines, Transactions of the ASME, Vol. 121, pp. 604-609, 1999.
4. Doyle Jay Orr Jr., Macro-Scale Investigation of High Speed Gas Bearings for MEMS Devices, Ph. D Thesis of MIT, 2000.
5. Development of Micro Gas Turbine System, 1st year Technical Report at KIST.
6. Mohamed Gad-el-Hak, The Fluid Mechamics of Microdevices The Freeman Scholar Lecture, Journal of Fluids Engineering, Vol. 121, pp. 5-33, 1999.
7. Hamrock, Fundamentals of Fluid Film Lubrication, McGraw-Hill,International Editions, 1994.